IJCRT.ORG ISSN : 2320-2882

INTERNATIONAL JOURNAL OF CREATIVE RESEARCH THOUGHTS (IJCRT)

An International Open Access, Peer-reviewed, Refereed Journal

COMPARITIVE ANALYSIS ON SINGLE PHASE DOUBLE STAGE GRID CONNECTED PV SYSTEM OPERATING UNDER FULLY SHADED CONDITION

[1]G. Manikanta, [2]N. Prema Kumar

[1]M. Tech Scholar, [2] Professor & Head of the department, EE, AUCEW

[1] Electrical Engineering Department,

[1]Andhra University College of Engineering, Visakhapatnam, India

Abstract: In recent times, there has been a notable surge in the adoption of single-phase transformerless grid-connected Photovoltaic (PV) systems. This trend can be attributed to their reduced physical dimensions and volume, which in turn contribute to an augmented operational efficiency. The present study focuses on the successful implementation of a single-phase, two-stage grid-connected PV system,both under Standard Test Conditions (STC) and during load variations. The initial stage of this systemincorporates the utilization of DC-DC converters based on Maximum Power Point Tracking (MPPT) control. The MPPT algorithm employed encompasses the Perturb and Observe as well as the incremental conductance (INC) methods, which are harnessed to attain the utmost power output from the photovoltaic module. Moving to the subsequent stage, a DC-AC inverter is employed in conjunction with an LCL filter and a Phase Locked Loop (PLL). These components synergistically facilitate synchronization with the grid. An investigation has been conducted on a grid-connected solar power generation system of modest scale, boasting a maximum power output capacity of 2kW. The purpose of this analysis is to delve into the intricacies of its functioning. Through meticulous simulations, the outcomes substantiate the superior efficacy of the Incremental Conductance (INC) algorithm in terms of maximum power point tracking within the context of a grid-connected network, as compared to the traditional INC algorithm. Furthermore, the accomplishment of seamless grid current synchronization with grid voltage has been achieved, both during standard test conditions and varying load scenarios. These successful synchronization endeavours highlight the robustness of the system's design and its ability to adapt to different operational contexts. The cumulative findings collectively showcase the system's performance in a manner that is indeed satisfactory, instilling confidence in its capabilities andpotential for practical application.

Index Terms - Photovoltaic system (PV), Maximum Power Point Tracking (MPPT), Perturb and Observe (P&O) Incremental Conductance (INC), Phase Locked Loop (PLL).

I. INTRODUCTION

In the contemporary landscape, solar energy-based power systems have gained remarkable popularity, particularly for off-grid power generation endeavours. The installation of Photovoltaic (PV) systems, although entailing a substantial initial investment, offers the unique advantage of zero operational running costs. The efficacy of these PV systems is intricately tied to variables such as solar irradiance and temperature, which significantly impact their performance. The direct connection of panels to the load presents challenges due to

the inherent variability and unpredictability in generating energy from solar sources, predominantly stemming from the fluctuations in environmental conditions. This variability can be mitigated through the employment of Maximum Power Point Tracking (MPPT) methods, which strive to optimize power generation under varying conditions. The efficiency of solar cells hinges on a multitude of factors, encompassing temperature, insolation, spectral properties of sunlight, presence of dirt and shadows, among others. These factors collectively influence the current-voltage and power-voltage characteristics of the PV system and consequently impact the connected load. Solar energy stands as an attractive choice for power generation, given its direct conversion into electrical energy via solar photovoltaic modules. Nevertheless, PV generation systems encounter notable

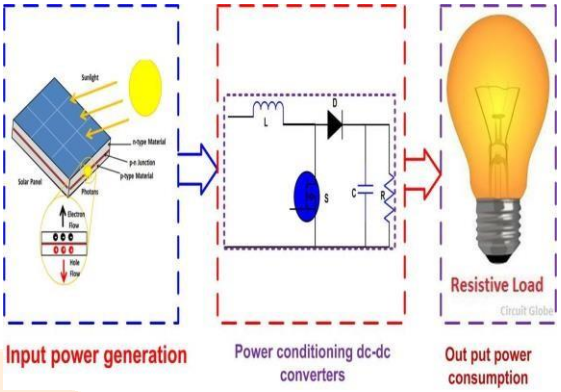

challenges. Conversion efficiency during power generation is relatively low, especially in conditions of limited irradiation. The generated electric power fluctuates continuously in response to weather dynamics. The nonlinear nature of solar cell Voltage-Current (V-I) characteristics, coupled withtheir susceptibility to irradiation and temperature changes, further complicates the system's behaviour.The integration of a converter with MPPT capability facilitates load matching and adherence to the maximum power transfer theorem, thereby optimizing the power generation process. A pivotal concernaffecting solar PV systems is the erratic availability of solar irradiances, a parameter with considerableinfluence on their output. The functionality of the power converter is intricately intertwined with the control methodology, aimed at stabilizing both the load and the power source in tandem. This control technique hinges on feedback from the load side, which is continuously compared against a reference value to ensure optimal operation of the DC-DC converter. To address the challenge of maintaining a consistent output voltage, an array of power electronic DC-DC converters is employed, replacing conventional circuits such as rheostats and potential dividers. However, this technique does result in a drawback: the output voltage obtained tends to be lower than the input voltage, leading to a reduction in overall efficiency. To address the issue of voltage stability and provide a dependable output, a rangeof power electronic converters are harnessed. In standalone PV systems, batteries play a crucial role instoring the harvested solar PV energy, ensuring a steady supply even during periods of low solar output.

Fig.1 DC-DC converter integration in HRES system

The Power-Voltage (P-V) characteristics of PV modules are typically represented by a single curve under conditions of uniform irradiance. Within this context, Perturb and Observe (P&O) as well as Incremental Conductance (INC) algorithms have gained prominence as frequently employed MPPT techniques due to their adept balance between performance and simplicity. An innovative enhancementto the P&O MPPT algorithm is introduced, aimed at achieving drift-free operation. Moreover, an MPPTalgorithm characterized by exceptional efficiency and swift tracking capabilities, particularly during rapid irradiation changes, has been proposed. The focal point of this study introduces a single-phase 2098W PV system designed for grid-connected applications. This system operates under Standard TestConditions (STC) and features diverse DC-DC Converters, both isolated and non-isolated. The endeavour involves the injection of a sinusoidal current, harmonized with the grid voltage, into the power grid through the implementation of an H-bridge inverter equipped with an LCL filter and PhaseLocked Loop (PLL) technology. This holistic approach embodies an intricate interplay of various components and advanced control strategies to ensure seamless integration and optimal operation within the grid-connected PV system.

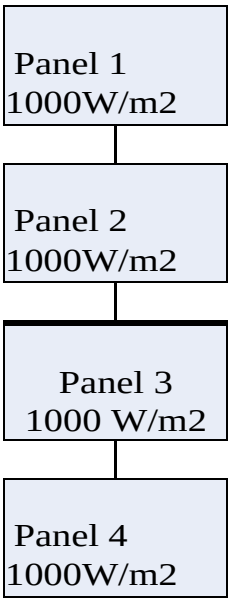

Fig.2 PV array with four series connected modules under fully shaded condition.

The state of a photovoltaic (PV) array being under fully shaded conditions denotes a scenario in whichthe incident irradiation stands at 1000 watts per square meter, accompanied by a temperature of 25 degrees Celsius. This particular set of parameters is commonly referred to as the standard test conditionwithin the realm of PV systems and solar energy research.

II. CONFIGURATION OF THE SYSTEM

The electric current and voltage sourced from the Photovoltaic (PV) array are directed into the utility grid through the intermediation of the Maximum Power Point Tracking (MPPT) controller and the DC-DC boost converter.

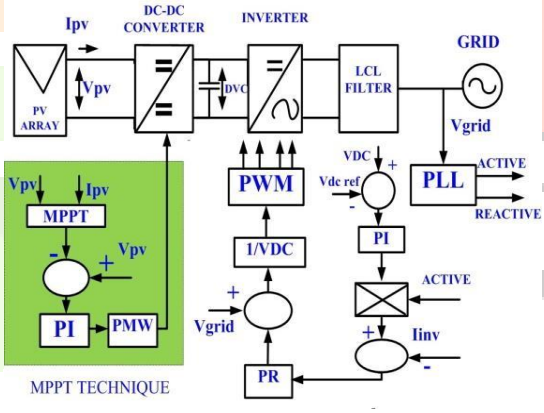

Fig.3 General Configuration of the Proposed PV System.

In the pursuit of optimizing energy extraction from the Photovoltaic (PV) array, a strategic adjustmentof the duty ratio in the boost converter is orchestrated to seamlessly align with the characteristics of theMaximum Power Point Tracking (MPPT) controller and the load and source impedance. The MPPT algorithm, encompassing Perturb and Observe (PO) as well as Incremental Conductance (INC) methodologies, is harnessed to continuously track and ascertain the most favourable duty ratio under Standard Test Conditions (STC). At the outset, the input voltage is maintained at an unregulated level of 250V, while the output voltage of the boost converter is meticulously regulated to a constant 400V.This configuration is deliberately designed to ensure a steady and reliable output voltage of 400V. As the meticulously regulated 400V DC voltage emerges from the boost converter, it undergoes a seamlesstransition into the subsequent phase of the process. This involves its integration into a single-phase DC-AC inverter, a key component in this intricate setup. The output of this inverter, after accounting for losses, achieves a peak voltage of 325V. To refine the output waveform and eliminate the direct current (DC) content, an LCL filter is judiciously employed. This filtering process culminates in the generation of a pure sine wave characterized by a frequency of 50 Hz and a voltage magnitude of 230V. This pristine waveform is then seamlessly injected into the utility grid, effectively contributing to the broader

energy ecosystem. The intricate orchestration of these components, algorithms, and control strategies culminates in a streamlined energy conversion process, ultimately channelling the potential of the PV array into a harmonious and productive relationship with the utility grid.

Figure 4 provides a comprehensive visual representation of the overarching structure that defines the proposed double-stage grid-connected photovoltaic system configuration. To ensure harmonious integration with the grid, a Phase Locked Loop (PLL) is judiciously implemented on the grid side, facilitating the synchronization of the inverter's operation with the dynamic grid environment.

Within the broader context, the Photovoltaic (PV) module emerges as a composition of numerous PVcells, each interlinked in a manner that could encompass both series and parallel configurations. Theunderlying mathematical framework outlining this intricacy is captured in Figure 4, offering a visual representation of the module's behaviour. Here, the symbols employed convey distinct parameters:

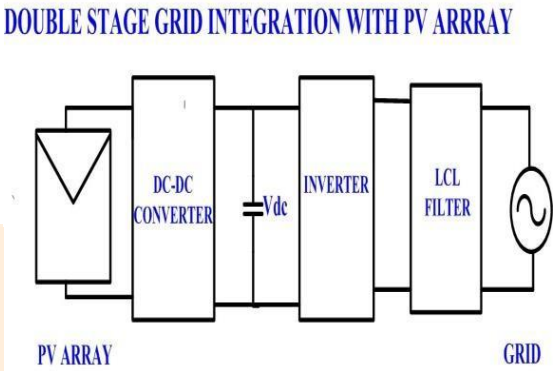

Fig.4 Double Stage Grid Integration with PV Array

"I" denotes the output current from the PV array, while "V" signifies the PV cell's output voltage. The variable "Iph" is representative of the photo current generated by the cell, its magnitude intricately tied to the incident solar irradiation. In a parallel fashion, "Ish" embodies the reverse saturation current of the cell, primarily influenced by the prevailing temperature conditions. As the numbers of series strings and parallel strings within the PV array manifest, they are aptly symbolized as "Ns" and "Np," respectively, ultimately defining the structural framework of the photovoltaic module. This intricate interplay of interconnected cells within the array

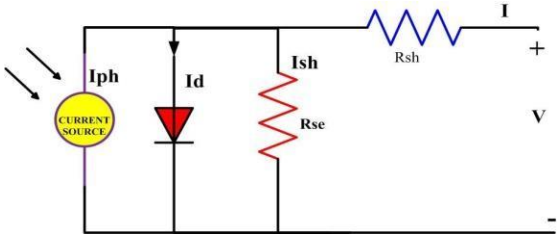

contributes to the dynamic energy production process, further underscoring the multifaceted nature of the proposed grid-connected photovoltaic system

Fig.5 Practical Equivalent Circuit of PV Cell

$$I = I_{ph} - I_D - I_{sh}$$

Where I= Output current of PV cell,

I_{ph} = Photo generated current,

I_D = Diode current,

I_{sh} = Shunt current

According to the principles encapsulated within the Shockley diode equation, the flow of current that undergoes diversion through the diode can be elegantly conceptualized and expressed in the followingmanner:

$$I_D = I_o(\exp(\frac{q(v+IR_s)}{mKT_c}) - 1)$$

Nevertheless, it is essential to delve into the intricate realm of mathematical representation when attempting to capture the current flowing within a Photovoltaic (PV) cell, aligning with the conceptualmodel, which can be elegantly articulated as follows:

$$I_D = I_{ph} - I_o(\exp(\frac{q(v+IR_s)}{mKT_c}) - 1) - \frac{v+IR_s}{R_{sh}}$$

Within the realm of Photovoltaic (PV) modules, two prominently recognized models have garnered attention: the single-diode model and the double-diode model. For the purpose of crafting a solar panelmodel that stands as a true representation of its intricate behaviour, the double-diode model emerges asa compelling choice. This sophisticated model ingeniously integrates the single-diode model, a choice attributed to its elegant balance between simplification and precision. By thoughtfully amalgamating the advantageous traits of these models, a more comprehensive and nuanced understanding of the solarpanel's operational dynamics can be effectively achieved.

$$I_{mp} = I_{ph} - I_o(\exp(\frac{q(v_{mp}+I_{mp}R_s)}{mKT_c}) - 1) - \frac{v_{mp}+I_{mp}R_s}{R_{sh}}$$

Where I_{mp} = maximum panel current,

v_{mp} = maximum panel voltage.

I. MAXIMUM POWER POINT TRACKING

This section delves comprehensively into the theoretical underpinnings and functional intricacies of "Maximum Power Point Tracking" (MPPT), as it pertains to its application within the domain of solar electric charge controllers. Within this discourse, the MPPT, recognized as the acronym for maximumpower point tracker, emerges as an innovative DC-to-DC converter, orchestrating the optimization of the symbiotic connection between the solar array, commonly referred to as photovoltaic (PV) panels, and the battery bank or the broader utility grid. This intricate mechanism, essentially, harmonizes the higher voltage direct current (DC) output generated by solar panels, with select instances from wind turbines, by elegantly transforming it into the requisite lower voltage magnitude, thus facilitating the precise charging of batteries. The interplay of these convergent technologies encapsulates an advanced facet of energy conversion and optimization that holds profound implications for harnessing solar energy's potential to its fullest extent.

(A) Perturb and Observe (P&O) MPPT

The elegance of the Perturb and Observe (P&O) MPPT technique lies in its innate simplicity and the seamless adaptability to various microcontrollers, rendering it a user-friendly choice for a multitude of applications. This pervasive usability prompts many researchers and practitioners to seamlessly integrate it into their ventures. As substantiated through an in-depth literature review, this methodologyis rooted in a trial-and-error paradigm, where the pursuit of the Maximum Power Point (MPP) involvesiterative adjustments. This technique finds its foundation in a power-versus-voltage (P-V) curve, with its computations commencing by contrasting the power yielded at two distinct points along the curve, alongside their respective voltage positions. This computational approach leads to the fine-tuning of voltage in an effort to trail the elusive MPP, a shift that might unfold on either side of the P-V curve. At its core, this strategy hinges on detecting changes in photovoltaic (PV) cell power, characterized by the differential parameter "dP," closely followed by an assessment of the voltage fluctuation denoted as"dV." The subsequent alteration in the duty cycle, "D," is dictated by the values derived from this interplay. The dynamic trajectory of the operating point's movement is meticulously traced using data derived from the P-V curve. This meticulous process unravels a profound insight: when the ratio (dP/dV) demonstrates positivity, the operating point inherently gravitates towards the left side of the MPP.

Conversely, when (dP/dV) assumes a negative value, it signifies alignment with the right half ofthe MPP. Iterative application of this methodology persists until the equilibrium point is achieved, marked by a state where (dP/dV) converges to zero. This intricate interplay of iterative computations within the dynamic context of power and voltage nuances represents the bedrock of the Perturb and Observe MPPT technique, embodying both its elegance and inherent complexities.

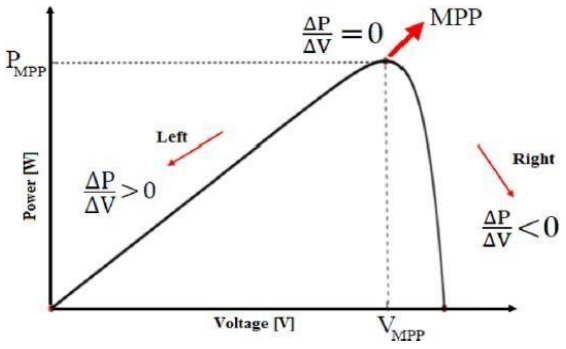

Fig.6 Behaviour of Solar panel indicating MPPT

MPP is given at the extreme point in any PV curve in order to determine MPP's position either left or right

$$\frac{\Delta P}{\Delta V} > 0 \quad \text{(left side of the MPP)}$$

$$\frac{\Delta P}{\Delta V} < 0 \quad \text{(right side of the MPP)}$$

$$\frac{\Delta P}{\Delta V} = 0 \quad \text{(at MPP)}$$

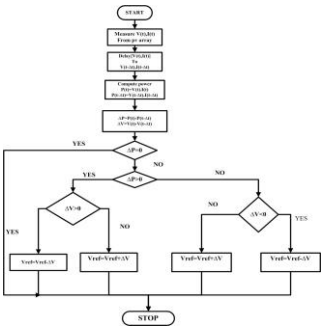

Fig.7 P&O Algorithm

B) INCREMENTAL CONDUCTANCE MPPT

This approach capitalizes on the fundamental principle that the slope of the photovoltaic (PV) curve atthe maximum power point (MPP) becomes mathematically equivalent to zero, signifying a critical point of equilibrium between power generation and voltage-current dynamics. Furthermore, when examiningthe slopes to the left and right of the MPP, it becomes apparent that the slope on the left assumes a positive value, denoting a surplus of generated power as voltage decreases, whereas the slope on the right takes a negative value, indicating a surplus of power as voltage increases.

Through a meticulous comparison of the instantaneous and incremental conductances, characterized bythe ratios of current to voltage (I/V) and the changes in current to changes in voltage (ΔI/ΔV) respectively, the tracking of the MPP is methodically executed. This method effectively navigates the intricate terrain of photovoltaic performance optimization, ensuring that the system efficiently harnesses the available solar energy.

The mathematical approach for calculating the position of MPPon the P-V curve is given by P=V*I

Using chain rule for the derivatives of the product, $\frac{\Delta P}{\Delta V} = \frac{\Delta t}{\Delta v}$

$$= I(\frac{\Delta V}{\Delta V}) + V(\frac{\Delta t}{\Delta v})$$

$$= I(1) + V(\frac{\Delta t}{\Delta v})$$

$$\frac{1}{v}(\frac{\Delta p}{\Delta v}) = \frac{1}{v}(\frac{\Delta t}{\Delta v})$$

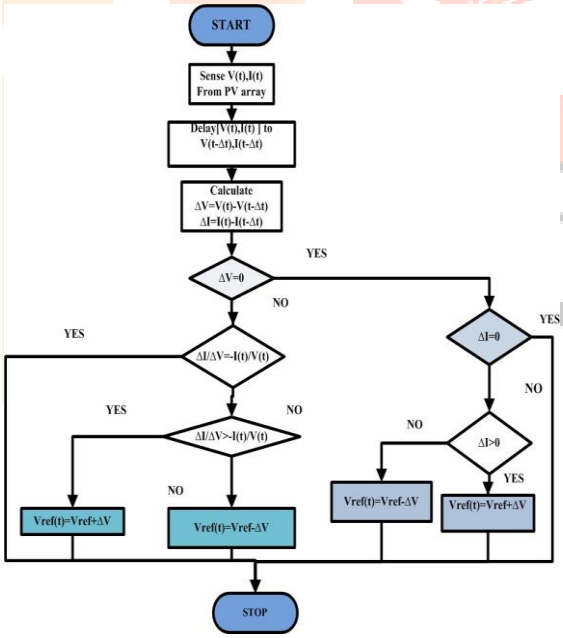

Fig.8 Flowchart of the INC algorithm

The formulation of the incremental conductance algorithm involves a comprehensive process of differentiation, where the output power of the Photovoltaic (PV) module is systematically differentiated concerning the voltage parameter. This multifaceted operation is orchestrated to yield a nuanced understanding of the intricate relationship between power and voltage dynamics. The pivotal aim of this differentiation endeavor lies in achieving a state of equilibrium, wherein the derivative outcome is set precisely to zero.

This mathematical maneuver is inherently geared towards identifying the precise voltage point at which the crucial balance between power generation and voltage profile reaches its pinnacle, encapsulating the essence of the incremental conductance algorithm's theoretical foundation.

$$\frac{\Delta I}{\Delta V} \geq -(\frac{I}{V})$$ (left side of the MPP)

$$\frac{\Delta I}{\Delta V} \leq -(\frac{I}{V})$$ (right side of the MPP)

$$\frac{\Delta I}{\Delta V} = -(\frac{I}{V})$$ (at MPP)

IV. PROPOSED CONVERTERS

A) BOOST CONVERTER

The Boost converter, renowned for its distinctive attribute as a step-up converter, orchestrates a voltage elevation at the output facet through the adept utilization of a switch mode power supply mechanism. Embedded within its architecture is an energy storage component, which could manifest as a capacitor or an inductor. This pivotal energy-storing element plays a crucial role, positioned either at the input or output terminus, functioning primarily as a filter to enhance overall operational stability. For the purpose of curbing output voltage perturbations to their minimal extent, a judiciously sized capacitor denoted as "C" assumes paramount significance. The chosen value of "C" should be substantially high to ensure effective voltage ripple reduction.

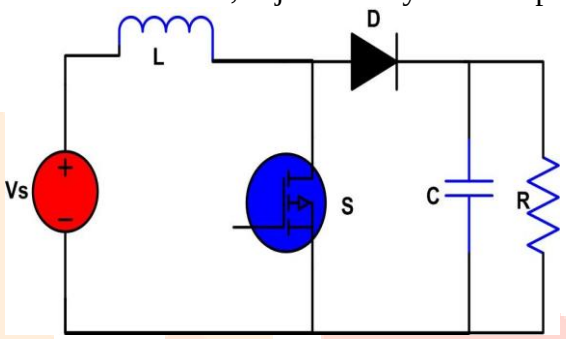

Fig.9 DC-DC Boost Converter

The semiconductors operating as switches within this intricate framework typically encompass a repertoire of choices, spanning the likes of MOSFET, IGBT, and BJT. The switching dynamics are orchestrated as follows: Upon the activation of Switch "S," an orchestrated current flow courses through the inductor, subsequently permeating through the switch, and finally reconnecting with the source to confer a charging effect upon the inductor "L." In a reciprocal fashion, when the switch transitions into a short-circuit state, the output voltage across the circuit promptly dwindles to zero.

The subsequent stage of the operation transpires as the switch is purposefully disengaged ("OFF" position). In this phase, the inductor undergoes a polarity reversal, initiating a process of discharge. This discharge trajectory unfolds through a progression from Vs (source voltage), Inductor "L," diode "D," the connected load, and concludes with a return to the source voltage, Vs. Guided by the synergistic interplay of the supply voltage and the action of the inductor "L," this orchestrated flow amplifies voltage magnitude at the output terminal. This augmentation is the cumulative result of the original supply voltage's contribution and the unique effect exerted by the inductor's inherent action. To encapsulate the essence of the Boost converter: it stands as an ingeniously conceived step-up converter, employing the sophisticated methodology of switch mode power supply to effectively elevate the voltage profile at the output juncture. A vital element contributing to its operational finesse is the presence of capacitors strategically situated either at the input or output section, playing an instrumental role in filtering and attenuating potential disturbances. Akin to the earlier discourse, the pursuit of minimized output voltage perturbations underscores the significance of a robustly sized capacitor. Across various implementations, the versatile selection of MOSFETs, IGBTs, or BJT semiconductors as switches remains a consistent theme, reflecting the adaptability of these components within the dynamic ecosystem of the Boost converter.

The output voltage of the boost converter is given as:

$$V_o = \frac{V_s}{1-D}$$

D = on time duration of switch/ total switching time period

$$D = \frac{V_o - V_s}{V_o}$$

The value of filter inductance is given as:

$$L = \frac{V_S * D * T}{\Delta I_L}$$

Filter capacitance C is given as:

$$C = \frac{I_o * D * T}{\Delta V_o}$$

B) ZETA CONVERTER

The Zeta converter exhibits a resemblance to the Buck-Boost converter in its operational characteristics. This converter's output voltage can either be lower or higher than the input voltage, contingent upon the duty-cycle parameter (D) governing its operation. Notably, the Zeta converter assumes the classification of a fourth-order system type, a classification attributed to its utilization of energy storage components within its design. Specifically, the converter incorporates a pair of inductors and two capacitors, effectively generating an output voltage that corresponds to the non-inverted form of the input voltage waveform.

This converter manifests an inherent versatility across a spectrum of load resistance values, rendering it suitable for a wide array of applications. In the context of this analysis, it becomes evident that the Cuk, Sepic, and Zeta converters are outcomes of intentional alterations to the arrangement of passive components within the foundational Buck-Boost converter. These modifications culminate in distinct converter architectures that serve specific operational purposes, thereby underlining the profound influence of component positioning on the converters' overall functionality and application scope.

$$D = \frac{V_o}{V_o + V_s}$$

Where D= on time duration of switch/total switching time period.

Output Voltage of the Zeta converter is given as:

$$V_o = V_s\left(\frac{D}{1-D}\right)$$

The value of filter inductance is given by:

$$L_1 = \frac{V_s * D}{\Delta I_1 * f}$$

$$L_2 = \frac{V_s * D}{\Delta I_2 * f}$$

The value of filter capacitance is given by:

$$C_1 = \frac{I_o * D}{\Delta V_{c1} * f}$$

$$C_2 = \frac{V_s * D}{\Delta V_{c2} * f^2 * 8 * L_2}$$

Where f= switching frequency,

ΔI_1 = peak to peak ripple current I_1,

ΔI_2 = peak to peak ripple current I_2

ΔV_c = voltage ripple,

D = Duty cycle.

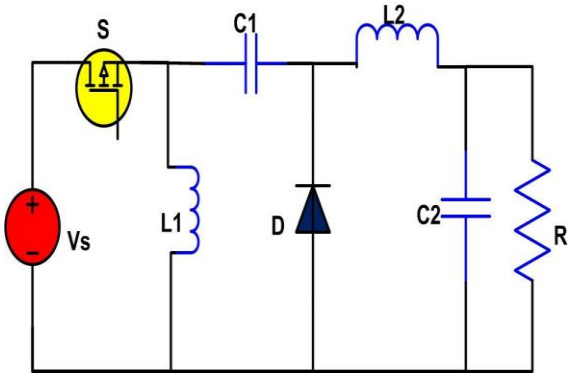

Fig.10 Zeta Converter

V. DC-AC CONTROL FOR THE GRID CONNECTED PV INVERTER

A Phase-Locked Loop (PLL) stands as a pivotal instrument harnessed to orchestrate an intricate synchronization dance between the voltage output of an inverter and the voltage prevalent in the utility grid. This harmonious coordination is achieved through the dexterous extraction of the phase angle characterizing the grid voltage, which in turn facilitates the calculated determination of the grid current's behaviour. Orchestrating this symphony, the controller steps onto the stage, conducting the grid current (ig) with precision and finesse. The controller's directives are intricately aligned with a reference emanating from the voltage controller, setting the stage for a performance of utmost synchrony.

The role of the H-bridge inverter assumes prominence as it emerges as a conduit channelling the harnessed power into the utility grid. This feat is accomplished by meticulous modulation of the DC link voltage (Vdc), which in turn becomes the artist's brushstroke dictating the flow of extracted energy. Yet, to elevate the output waveform to the pinnacle of purity, a filter circuitry steps forth, embodying an artful endeavour to cast away the unwanted harmonics permeating the inverter's sonic creation. Within this endeavour, a transformation occurs, birthing a sine wave of impeccable integrity and standing tall with an amplitude valiantly poised at 325 V.

Contemplating the domain of filters, a triumvirate of prototypes - the L, LC, and LCL filters - emerges into the limelight, each a contender vying to don the crown of excellence. Amidst this contest, the LCL filter emerges as the virtuoso, its performance exceeding that of its peers. Its secret lies in its ability to seize the majority of harmonics, thereby elevating its essence to that of a harmonious purifier. In the context of the grander narrative, the LCL filter finds itself a suitable companion to grid-connected Photovoltaic (PV) systems, a fitting synergy that underscores its unmatched prowess in this realm. Thus, a portrayal of the inverter takes form, depicting an ingeniously devised entity poised to traverse the landscape of energy conversion. At its core, the inverter emerges as an electronic protagonist endowed with the ability to metamorphose a direct current's essence into an asymmetrical alternating current, a transformation governed by precision and intent, orchestrated to unravel a symphony characterized by the interplay of magnitude and frequency.

Within the expansive realm of power electronics, the intricate domain of inverters unfolds into a tapestry woven from two primary classifications, each bearing its own distinct imprint on the landscape: the line-commutated inverters and the self-commutated inverters. Yet, even within this binary demarcation, the inverter landscape further unfurls into a myriad of sub-categories, akin to constellations adorning the night sky, each embodying

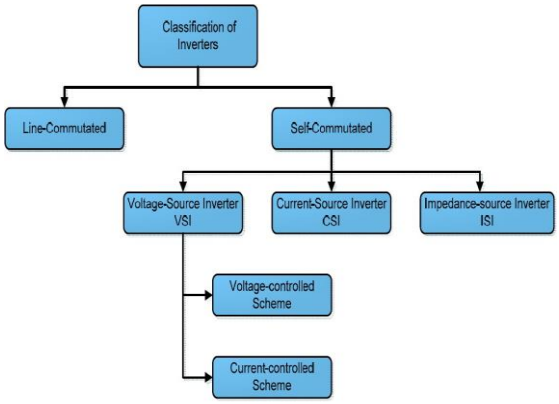

a unique facet of functionality and application.

Fig.11 Classification of Inverters

This grand taxonomy of inverters is sculpted by various dimensions, a multidimensional space where the types of input sources converge with the nuances of output characteristics. In this symphony, the interplay of connection methods harmonizes with the diversity of load types, each chord resonating with its own purpose

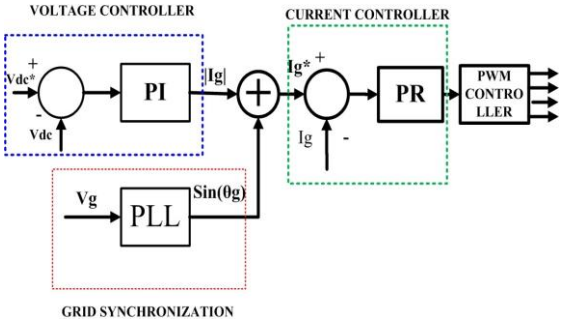

and utility.

Fig.12 Inverter Control Circuit

The Line-Commutated Inverter (LCI) operates under the influence of grid parameters that dictate its commutation process. It necessitates additional circuitry to activate switching devices. In contrast, the Self-Commutated Inverter (SCI) is a fully controllable entity, guided entirely by the potential at its gate terminal. This programmable nature empowers the SCI to govern both current and voltage waveforms at the inverter's output. The SCI finds optimal application in Grid-Connected Photovoltaic (GPV) systems, boasting robustness against grid disruptions and adeptness in mitigating current harmonics. This quality, in turn, enhances the overall quality of grid power.

CONTROL MECHANISM FOR GPV SYSTEM:

To achieve full suppression of the Source Side Harmonics (SSE) in grid current and attain a refined Sine Pulse Width Modulation (SPWM) signal, a Proportional Resonant (PR) controller is preferred over another type of controller. The PR controller's resilience against disturbances and its generation of sinusoidal reference waveforms are harnessed through the use of infinite gain. The grid synchronization methodology proves advantageous in dual aspects. Firstly, it not only reproduces a filtered signal in sync with the grid voltage, but also replicates an orthogonal grid voltage component, which becomes the foundation for initializing the generation of reactive power references for the inverter. Consequently, the inverter gains the capability to manipulate reactive power flow, diverging from traditional inverters that solely handle active power transfer due to their inability to generate the orthogonal current reference component. Secondly, for the Synchronous Reference Frame Phase-Locked Loop (SRE-PLL) to synchronize with the grid voltage phase, the integration reset and d-q transformations necessitate zero-voltage crossing detection, thereby entailing sine and cosine calculations.

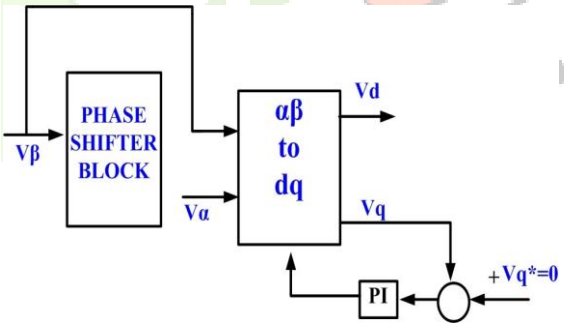

Fig.13 Single phase SRF-PLL for Grid Synchronization.

VI. RESULTS & DISCUSSIONS

Both the P&O and INC algorithms were simulated under the same operating conditions, each with a simulation time of 3.5 seconds and a duty ratio of 0.355. The settling time for the P&O method was measured at 0.765 seconds, while the INC algorithm exhibited a faster settling time of 0.485 seconds. Notably, the P&O method displayed a longer settling time compared to the INC method. Moreover, losses incurred by the P&O algorithm were higher, amounting to 13.5W, whereas the INC algorithm exhibited lower losses, measuring 11W. Both scenarios maintained a DC Link voltage of 400V, yet it's worth highlighting the significantly shorter settling time achieved by the INC algorithm. An in-depth comparative examination encompassing various Maximum Power Point Tracking (MPPT) techniques in conjunction with a double-stage grid integration framework is undertaken to discern their nuances, advantages, and potential synergies.

Parameters are to be considered as:
Switching Frequency of the converter= F_s=5Khz
Switching Frequency of the inverter=F_s=10Khz
Input voltage= 250V,
Output Voltage of DC link Capacitor=400V,
Grid voltage = 230(RMS),
Grid Frequency= 50Hz,
Converter change in current ripple=5%,
Change in Voltage Ripple=1%,
PV Array=2KW (1 Soltech STH=350WH),
Series connected modules per string= 6;
Parallel string=1,
Inverter Side Inductance L_1=4.36mH,
Grid Side Inductance L_2=4.81mH,
Filter side Capacitance = 6.21microF

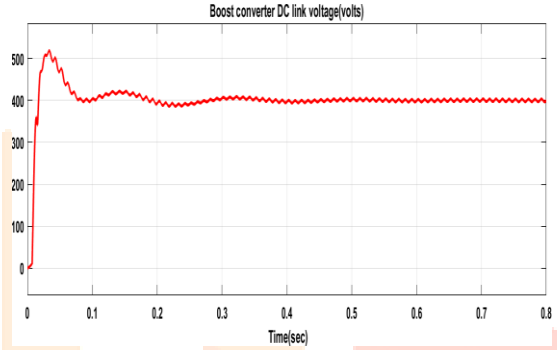

Fig.14 Simulation result of DC link Boost voltage(P&O)

The above figure shows variation of DC link voltage with respect to time. The DC link voltage settles to a value of 400V after time equal to 0.35sec.

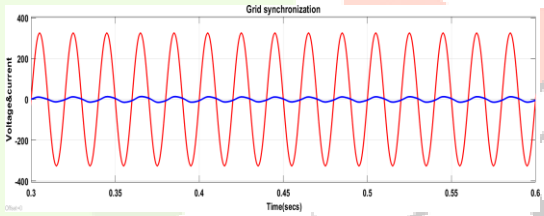

Fig.15 Simulation result of Grid synchronization with active component(P&O)

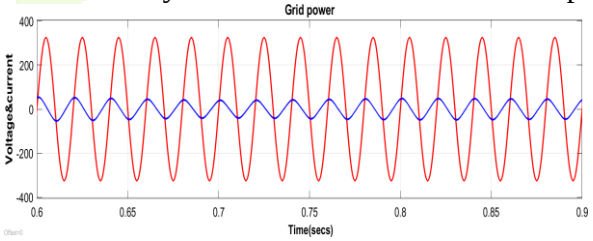

Fig.16 Simulation result of Grid synchronization with reactive component(P&O)

It shows variation of voltage and current with respect to time. It can be observed that reactive power feeding to the Grid with Peak to peak output voltage value is 325V and output current value is 13A.

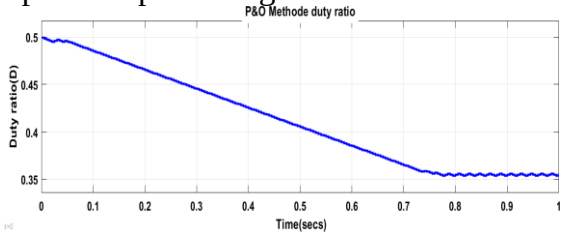

Fig.17 Simulation result of Duty Cycle(P&O)

It shows variation of duty cycle with respect to time. The settling time is 0.765 sec.

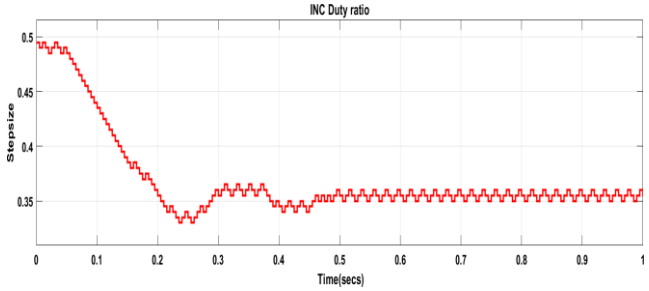

Fig.18 Simulation result of duty cycle (INC)

The above fig. shows the variation of duty cycle w.r.t time. The settling time is 0.465sec with a duty ratio of 0.355.

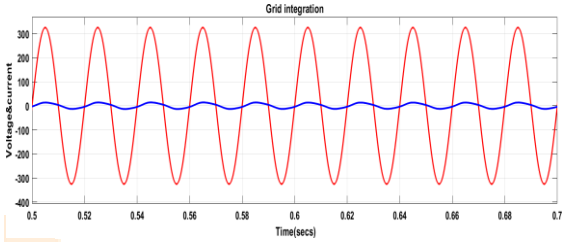

Fig.19 Simulation result of Grid synchronization with active component (INC)

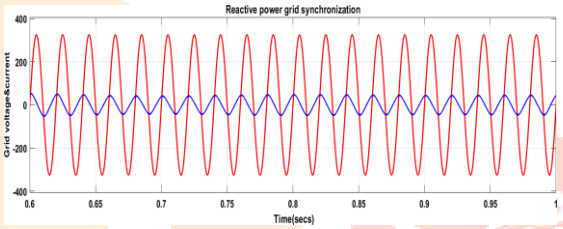

Fig.20 Simulation result of Grid synchronization with reactive component (INC)

It shows variation of voltage and current with respect to time. It can be observed that reactive power

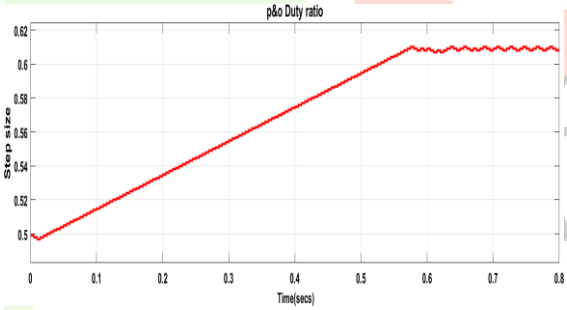

feeding to the Grid with Peak to peak output voltage value is 325V and output current value is 13A.

Fig.21 Simulation result of Duty ratio of zeta converter (P&O)

It shows the variation of duty cycle w.r.t time. The settling time is 0.675sec and duty ratio is 0.61sec.

Fig.22 Simulation result of output power for zeta converter(P&O)

It shows the variation of grid power w.r.t time. The settling time is 0.675sec. the value of grid power is 1874W.

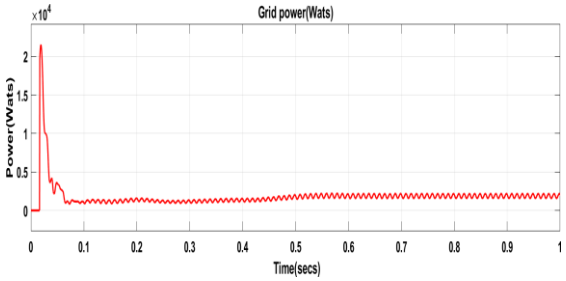

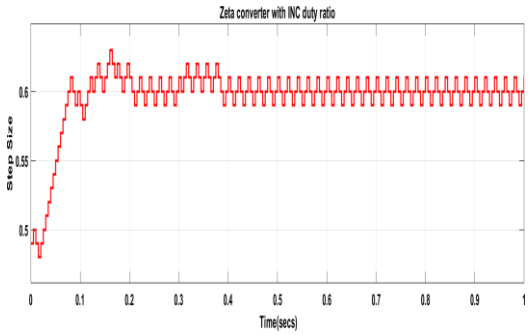

Fig.23 Simulation result of duty ratio for Zeta converter (INC)

It shows the variation of duty cycle w.r.t time. The settling time is 0.37sec with duty cycle value 0.61.

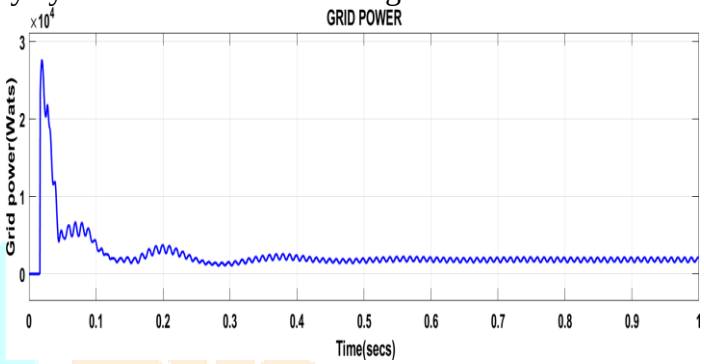

fig.24 Simulation result of output power of zeta converter (INC)

It shows variation of output power w.r.t time. The settling time is 0.37sec. the grid power value is 1814W.

Table.1: A Comparative analysis of MPPT techniques with Double stageGrid integration.

Converter	MPPT tech-niques used	Settling time	Duty ratio	DC link Volt-age	Input power (W)	out power (W)	losses (W)	Effici ency
Boost	P&O	0.765 Sec	0.355	400	2094	2084.5	13.5	99.35%
Boost	INC	0.485 Sec	0.355	400	2090	2079	11	99.47%
Zeta	P&O	0.675 Sec	0.609	400	2092	1874	218	89.5%
Zeta	INC	0.37 Sec	0.6	400	2070	1814	180	89.87%

VII. CONCLUSION

The study investigates PV array integration with the grid employing perturb and observe (P&O) and incremental conductance (INC) algorithms alongside various converter configurations. Matlab simulations were conducted, exploring different converters with MPPT techniques. Boost converters emerged as the optimal choice, showcasing superior performance across metrics like efficiency, duty cycle, settling time, and component size. Efficiency reached 99.35% using P&O and 99.47% with INC. Additionally, the duty ratio proved to be 0.355, the lowest among all converters, and the converter demanded fewer components, minimizing spatial requirements.

Furthermore, grid voltage and grid current exhibited synchronization. Compared to other converters, the zeta converter presented higher voltage and current ripple. Between the P&O and INC MPPT methods, the INC technique demonstrated better efficiency and fewer steady-state oscillations.

REFERENCES

[1] Alajmi, B.N., Ahmed, K.H., Finney, S.J., Williams, B.W., 2013. A maximum power point tracking technique for partially shaded photovoltaic systems in microgrids. IEEE Trans. Ind. Electron 60, 1596–1606. http://dx.doi.org/10. 1109/TIE.2011.2168796.

[2] Pilakkat, D., Kanthalakshmi, S., 2019. Artificial Bee Colony Integrated P&O Algorithm for Single Phase Grid Connected Photovoltaic Application. International Journal of Instrumentation and Measurement

[3] Mohanty, S., Subudhi, B., Ray, P.K., 2016. A new MPPT design using grey Wolf optimization technique for photovoltaic system under partial shading conditions. IEEE Trans. Sustain. Energy 7, 181–188. http://dx.doi.org/10.1109/TSTE.2015.2482120

[4] Meraj ST, Yahaya NZ, Singh B, Singh M, Kannan R, Engineering E. Implementation of a robust hydrogen-based grid system to enhance pow- erquality. 2021;153–58.

[5] Khezri, R.; Mahmoudi, A.; Haque, M.H.H. Optimal Capacity of So- lar PV and Battery Storage for Australian Grid-Connected Households. IEEE Trans. Ind. Appl. 2020, 56, 5319–5329.

[6] Joisher, M.; Singh, D.; Taheri, S.; Espinoza-Trejo, D.R.; Poures- maeil, E.; Taheri, H. A Hybrid Evolutionary-Based MPPT for Photo- voltaic Systems Under Partial Shading Conditions. IEEE Access 2020, 8, 38481–38492.

[7] Karthikeyan, V.; Rajasekar, S.; Das, V.; Pitchaivijaya, K. Grid- Connected and Off-Grid Solar Photovoltaic System. Green Energy Tech- nol. 2017.

[8] Hamza, H.A.; Auwal, Y.M.; Sharpson, M.I. Standalone PV System De- sign and Sizing for a Household in Gombe, Nigeria. Int. J. Interdiscip. Res. Innov. 2018, 6, 96–101.

[9] Amir, A.; Amir, A.; Che, H.S.; Elkhateb, A.; Rahim, N.A. Comparative analysis of high voltage gain DC-DC converter topologies for photo- voltaic systems. Renew. Energy 2019, 136, 1147–1163.

[10] Senthilvel, A.; Vijeyakumar, K.; Vinothkumar, B. FPGA Based Imple- mentation of MPPT Algorithms for Photovoltaic System under Partial Shading Conditions. Microprocess. Microsyst. 2020, 77, 103011.

[11] Amir, A.; Amir, A.; Che, H.S.; Elkhateb, A.; Rahim, N.A. Comparative analysis of high voltage gain DC-DC converter topologies for photo- voltaic systems. Renew. Energy 2019, 136, 1147–1163.

[12] Zhang, R.;Wu, A.; Zhang, S.;Wang, Z.; Cang, S. Dynamical analysis and circuit implementation of a DC/DC single-stage boost converter with memristance load. Nonlinear Dyn. 2018, 93, 1741–1755.